

Generation of optical bottle beams by incoherent white-light vortices

Vladlen G. Shvedov^{1,2}, Yana V. Izdebskaya¹, Andrei V. Rode¹, Anton Desyatnikov¹, Wieslaw Krolikowski¹, and Yuri S. Kivshar¹

¹*Nonlinear Physics Center and Laser Physics Center, Research School of Physical Sciences and Engineering, Australian National University, Canberra ACT 0200, Australia*

²*Department of Physics, Taurida National University, Simferopol 95007 Crimea, Ukraine*

Abstract: We generate experimentally optical bottle beams from incoherent double-charge white-light vortices, and show that their parameters can be efficiently controlled by varying the beam focusing conditions.

© 2008 Optical Society of America

OCIS codes: (140.3300) Lasers and laser optics : Laser beam shaping, (140.7010) Lasers and laser optics : Laser trapping, (030.1640) Coherence and statistical optics : Coherence

References and links

1. A. Ashkin, J. M. Dziedzic, J. E. Bjorkholm, and S. Chu, "Observation of a single-beam gradient force optical trap for dielectric particles," *Opt. Lett.* **11**, 288-290 (1986).
2. K. Dholakia, P. Reece, and M. Gu, "Optical micromanipulation," *Chem. Soc. Rev.* **37**, 42-55 (2008).
3. A. Ashkin, "Acceleration and trapping of particles by radiation pressure," *Phys. Rev. Lett.* **24**, 156-159 (1970).
4. T. Kuga, "Novel optical trap of atoms with a doughnut beam", *Phys. Rev. Lett.* **78**, 4713-4716 (1997).
5. A. Ashkin, "History of optical trapping and manipulation of small-neutral particle, atoms, and molecules", *IEEE J. Sel. Top. Quantum Electron.* **6**, 841-856 (2000).
6. D. G. Grier, "A revolution in optical manipulation", *Nature* **424**, 810-816 (2003).
7. H. Rubinsztein-Dunlop, T. A. Nieminen, M. E. J. Friese, and N. R. Heckenberg, "Optical trapping of absorbing particles," *Adv. Quantum Chem.* **30**, 469-492 (1998).
8. R. Ozeri, "Large-volume single-beam dark optical trap for atoms using binary phase elements", *J. Opt. Soc. Am. B* **17**, 1113-1116 (2000).
9. J. Arlt and M. J. Padgett, "Generation of a beam with a dark focus surrounded by regions of higher intensity: the optical bottle beam", *Opt. Lett.* **25**, 191-193 (2000).
10. N. Bokor and N. Davidson, "A three dimensional dark focal spot uniformly surrounded by light", *Opt. Commun.* **279**, 229-234 (2007).
11. P. Rudy, R. Eijnisman, A. Rahman, S. Lee, and N. P. Bigelow, "An all optical dynamical dark trap for neutral atoms," *Opt. Express* **8**, 159-165 (2001).
12. N. Friedman, L. Khaykovich, R. Ozeri, and N. Davidson, "Compression of cold atoms to very high densities in a rotating-beam blue-detuned optical trap," *Phys. Rev. A* **61**, 031403(R) -031406(R) (2000).
13. See, e.g., a comprehensive review paper, M. S. Soskin and M. V. Vasnetsov, "Singular optics," in: *Progress in Optics*, Vol. 42, Ed. E. Wolf (Elsevier, Amsterdam, 2001).
14. M. S. Soskin, P. V. Polyanskii, and O. O. Arkhelyuk, "Computer-synthesized hologram-based rainbow optical vortices," *New J. Phys.* **6**, 196 (2004).
15. G. Gbur and T. D. Visser, "Coherence vortices in partially coherent beams," *Opt. Commun.* **222**, 117-125 (2003).
16. M. E. J. Friese, T. A. Nieminen, N. R. Heckenberg, and H. Rubinsztein-Dunlop "Alignment or spinning of laser-trapped microscopic waveplates" *Nature* **394**, 348-350 (1998).
17. L. Allen, M. W. Beijersbergen, R. J. C. Spreeuw, and J. P. Woerdman, "Orbital angular momentum of light and the transformation of Laguerre-Gaussian laser modes," *Phys. Rev. A* **45**, 8185-8189 (1992).
18. A. I. Bishop, T. A. Nieminen, N. R. Heckenberg, and H. Rubinsztein-Dunlop, "Optical Microrheology Using Rotating Laser-Trapped Particles," *Phys. Rev. Lett.* **92**, 198104-198107 (2004).
19. M. Khan, A. K. Sood, F. L. Deepak, and C. N. R. Rao, "Optically driven nanorotors: Experiments and model calculations", *J. Nanosc. Nanotechn.* **7**, 1800-1803 (2007).
20. Y. Roichman, A. Waldron, E. Gardel, D.G. Grier, "Optical traps with geometric aberrations", *Appl. Opt.* **45**, 3425-3429 (2006).

21. R. K. Singh, P. Senthilkumaran and Kehar Singh, The effect of astigmatism on the diffraction of a vortex carrying beam with a Gaussian background J. Opt. A : Pure Appl. Opt. **9**, 543-554 (2007).
22. R. K. Singh, P. Senthilkumaran, K. Singh, "Focusing of a vortex carrying beam with Gaussian background by an apertured system in presence of coma", Opt. Commun. **281**, 923-934 (2008).
23. J. X. Pu, X. Y. Liu, and S. Nemoto, "Partially coherent bottle beams", Opt. Commun. **252**, 7-11 (2005).
24. J. X. Pu, M. W. Dong, and T. Wang, "Generation of adjustable partially coherent bottle beams by use of an axicon-len system," Appl. Opt. **45**, 7553-7556 (2006).
25. L. Rao, X. Zheng, Z. Wang, and P. Yei, "Generation of optical bottle beams through focusing J_0 -correlated Schell-model vortex beams", Opt. Commun. **281**, 1358-1365 (2008).
26. Z. M. Zhang, J. Pu, and X. Q. Wang, "Focusing of partially coherent Bessel-Gaussian beams through a high-numerical-aperture objective", Opt. Lett. **33**, 49-51 (2008).
27. A. Ciattoni, G. Cincotti, and C. Palma, "Circularly polarized beams and vortex generation in uniaxial media," J. Opt. Soc. Am. A **20**, 163-171 (2003).
28. A. V. Volyar and T. A. Fadeeva, "Generation of singular beams in uniaxial crystals," Opt. Spectrosc. **94**, 235-244 (2003).
29. V. Shvedov, W. Krolikowski, A. Volyar, D. N. Neshev, A. S. Desyatnikov, and Yu. S. Kivshar, "Focusing and correlation properties of white-light optical vortices," Opt. Express **13**, 7393-7398 (2005).
30. G. Gbur, T. D. Visser, and E. Wolf, "Hidden singularities in partially coherent and polychromatic wavefields," J. Opt. A **6**, S239-S242 (2004).
31. D. M. Palacios, I. D. Maleev, A. S. Marathay, and G. A. Swartzlander Jr., "Spatial correlation singularity of a vortex field", Phys. Rev. Lett. **92**, 143905-143908 (2004).
32. I. D. Maleev, D. M. Palacios, A. S. Marathay, and G. A. Swartzlander, "Spatial correlation vortices in partially coherent light: theory", J. Opt. Soc. Am. B **21**, 1895-1898 (2004).
33. T. van Dijk, G. Gbur, T.D. Visser, "Shaping the focal intensity distribution using spatial coherence," J. Opt. Soc. Am. A, **25**, 575-581 (2008).
34. M. Born and E. Wolf, *Principles of Optics* (Pergaman, Oxford, 1969).
35. S. A. Collins, "Lens-system diffraction integral written in terms of matrix optics", J. Opt. Soc. Am. **60**, 1168-1177 (1970).

1. Introduction

Trapping and manipulation of particles with optical tweezers was first demonstrated more than two decades ago [1] and it remains a very active field of research nowadays [2]. Optical tweezers [3, 4, 5, 6] utilize the gradient optical forces (or radiation pressure) to confine transparent particles as well as atoms, molecules, cells, colloidal suspensions, etc. Depending on the relative refractive index of a particle and the surrounding medium, the particles are trapped either in the intensity minima or maxima of the beam [7]. Typically, optical tweezers manipulate microscopic objects in a planar geometry, and the particles are confined in a thin layer defined by the focal area of the beam. In order to create an optical potential well and achieve fully three dimensional trapping, the so-called *optical bottle* have been proposed [3]. Latter on the term "optical bottle beam" was introduced to describe a beam with a finite axial region of low (and even zero) intensity surrounded in all dimensions by light [8, 9, 10]. Such bottle beams could be used to confine and transport a large number of particles or atoms [4, 8].

A number of different techniques has been proposed to generate bottle beams. This includes mechanical angular scanning of a laser beam [11, 12] and the use of optical diffractive elements such as holograms and phase plates to form a desired hollow axial structure. Many of these techniques involve *vortices*, i.e. optical beams carrying phase singularities. The vortex beam possesses a core with a vanishing intensity which coincides with the location of the phase singularity; the vortices are routinely generated by the use of phase masks, spiral phase plates, or spatial light modulators [13, 14, 15]. It has been shown that, similar to the optical spin momentum [16], the orbital angular momentum [17] carried by the vortex beam can be transferred to trapped particles inducing their rotation [18, 19].

Most of the realizations of optical tweezers and bottle beams employ coherent light being sensitive to phase distortions and leading to deterioration of the trapping [20, 21, 22]. This problem can be remedied by the use of light with partial spatial and temporal coherence. Re-

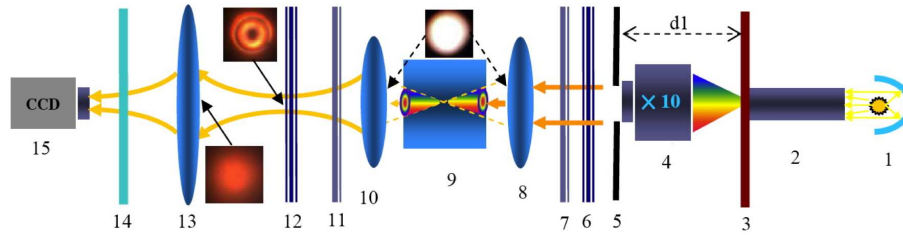


Fig. 1. Experimental setup: 1, halogen white-light source; 2, bundle of multi-mode optical fibers ($D=5\text{mm}$); 3, IR filter; 4, microscope objective; 5, aperture (2 mm); 6 and 12, polarizers; 7 and 11, achromatic quarter-wave plates; 8 and 10, collimation lenses; 9, uniaxial crystal (CaCO_3); 13, projection lens; 14, color filters; 15, color CCD.

cently, it was shown that focusing of the spatially *partially incoherent light* beam by an axicon leads to the formation of a bottle beam [23, 24]. Also, it was suggested that angular momentum-carrying bottle beam could be formed by using a partially coherent vortex beam [25, 26].

In this paper we demonstrate experimentally an efficient method for generating optical bottle beams by propagating a circularly polarized Gaussian beam through an uniaxial crystal and generating white-light incoherent optical vortices [27, 28, 29]. We study the intensity distribution and spatial correlation properties of the field inside the focal region and show that the size and shape of dark focus of the incoherent bottle beam is determined by the focusing conditions and the length of the uniaxial crystal.

2. Experimental generation of polychromatic incoherent optical bottle beam

Typically, optical vortices are generated by using holograms or spiral phase masks which upon transmission of light impose the desired helical phase structure [13]. Recently, we have demonstrated that white-light vortices can be generated by transmitting a circularly polarized beam through an uniaxial crystal [28, 29], and we employ this approach here.

The experimental setup is shown in Fig. 1. We use white light generated by a halogen lamp (power 50 W , angular divergence 8°) as a light source. The light from the lamp 1 passes first through the bundle of optical fibers 2 (with aperture 5 mm) and then through the infra-red filter 3 which results in the spectral range of $450 - 800\text{ nm}$. The beam is then collimated by the micro-objective 4 and aperture 5 acquiring almost Gaussian intensity profile. After the aperture the light passes through a polarizer 6 and achromatic $\lambda/4$ plate 7 attaining circular polarization. Subsequently, the beam is focused by lens 8 ($f = 50\text{ mm}$) onto an uniaxial calcite crystal 9 with the optical axis oriented along the beam propagation. During propagation through the crystal the polarization of the beam becomes elliptical with ellipticity depending on the distance. At the output of the crystal the light is collimated by a positive lens 10 ($f = 50\text{ mm}$) and then passes through another $\lambda/4$ plate 11 and polarizer 12. After adjusting the orientation of this polarizer, the outgoing beam acquires the structure of a linearly polarized double-charge incoherent optical vortex [27, 28, 29]. The vortex core size and the Rayleigh length of the beam are determined by the crystal length. In the experiments discussed here we use two crystals of different length, ($10 \times 10 \times 9\text{ mm}^3$) and ($10 \times 10 \times 1\text{ mm}^3$).

Earlier we demonstrated that the near-field intensity structure with on-axis dark region can be recovered by the beam focusing even after incoherence-induced vortex wash-out [29]. Here we use this feature for generating the bottle beams. The incoherent vortex beam propagates through the lens ($f=50\text{ mm}$) placed at the distance $d_2=170\text{ mm}$ from the collimator. After reaching the lens, the beam is spatially homogeneous and no vortex structure is visible (see Fig. 1) indicating its high degree of incoherence. The coherence radius in the image plane of the lens is evaluated

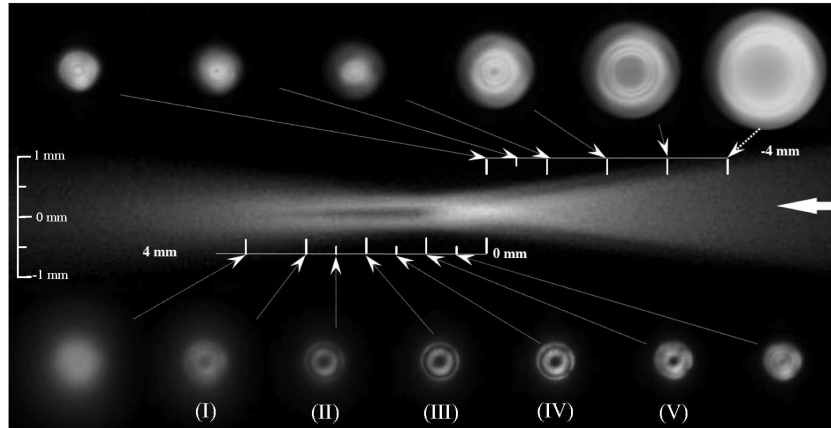


Fig. 2. Experimental longitudinal and cross-section distribution of intensity of particular coherence optical vortex near the focal region. The distance between the vortex formation plane and focusing lens ($f=50$ mm) is 170 mm. The dark core diameter for the labeled cross-sections is: I - $160\ \mu\text{m}$; II - $180\ \mu\text{m}$; III - $200\ \mu\text{m}$; IV - $200\ \mu\text{m}$; and V - $150\ \mu\text{m}$.

to be $\rho \approx 11\ \mu\text{m}$ which is much less than the diameter of the beam ($0.9\ \text{mm}$) making it virtually incoherent. The beam is then transmitted through the lens and evolves freely. It is well known that before reaching the focal caustic the vortex structure is not visible [30]. It starts to reappear in the focal region being fully recovered in the image plane (see Fig. 2). This effect points to a simple tool for recovering the hidden information about the vortex core, otherwise only available from the analysis of the cross-correlation function [31, 32].

The transverse spatial distribution of the light intensity of the focal caustic of the lens is registered by a CCD camera that can be translated along the beam axis. In order to observe the longitudinal cross-section of the generated bottle beams, we use a glass cuvette filled with 1% liquid solution of polystyrene nanoparticles ($50\ \text{nm}$ in diameter). When the beam propagates through the cuvette the side-mounted camera records the image produced by the transversely scattered light. Experimental results for 9 mm – long uniaxial crystal are shown in Fig. 2. The central part of this graph contains a side view of the light intensity distribution (bottle beam) while the insets depict its transverse cross-sections at the different axial locations.

The dark focal region surrounded by higher intensity light is a direct evidence of the incoherent bottle beam. By varying the degree of coherence we find that both transverse and longitudinal dimensions of the dark focal region increase with an increase of the correlation length of the incident light [33]. Moreover, we find that the light intensity surrounding the dark focus in the transverse and longitudinal directions increases and decreases with the decrease of the correlation length of the incident beams, respectively. As Fig. 2 shows, the size and shape of the dark focal area in the incoherent vortex beam depends on the vortex generation conditions. According to Ciattoni *et al.* [27] the longer the propagation of the Gaussian beam in an uniaxial crystal the higher the maximum intensity of the generated vortex. Furthermore, the effective energy conversion of the Gaussian beam into a vortex is higher for longer propagation distances. As a consequence, the length and transverse size of the dark area of the incoherent vortex bottle beam depends on the length of the uniaxial crystal.

In order to characterize the spatial structure of the experimentally created dark region of the bottle beam, we employ the measure of visibility for an optical vortex in the incoherent beam defined in the following way: for a given two-dimensional image of the beam cross-section we record a number ($n = 1, 2 \dots N$) of the radial intensity profiles. Then, from each profile we find

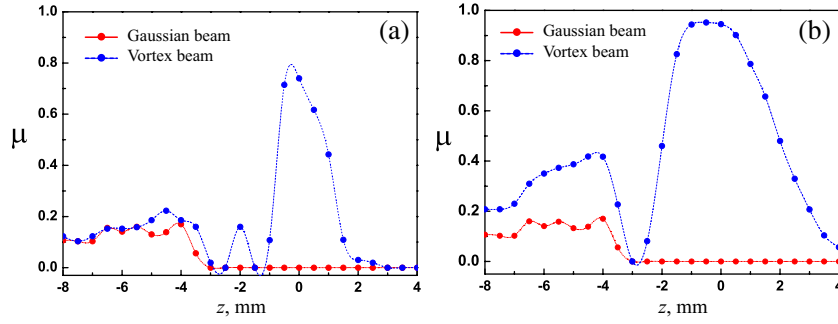


Fig. 3. Experimentally measured visibility of the bottle beam for the waists (a) $w_0 = 0.3$ mm (9 mm crystal) and (b) $w_0 = 0.2$ mm (1 mm crystal); source image plane is at $z = 0$.

the maximal, I_n^{\max} , and minimal, I_n^{\min} , values of intensity in the central part of the beam and evaluate the visibility as $\mu = 1 - 2 \sum^N I_n^{\min} / \sum^{2N} I_n^{\max}$. This quantity represents the averaged light intensity modulation in the vicinity of the beam axis. In the case of a perfect vortex with $I_n^{\min} = 0$ we have $\mu = 1$, whereas for the Gaussian beam $\mu = 0$ because $I_n^{\min} = I_n^{\max}$. In Fig. 3 (a) we plot the visibility vs. longitudinal coordinate z obtained from the bottle cross-sections in Fig. 2 (blue lines) and compare it with visibility for the Gaussian beam (red lines). As clearly seen in Fig. 3, the dark area of the vortex generated in a 9 mm – calcite crystal is 3 mm long (a), while for the 1 mm crystal the size of the dark area is 7 mm (b).

3. Theoretical analysis

We represent the electric field of a coherent monochromatic vortex in the standard form, $E_t = E_0 \left(r^{|l|} / w_0^{|l|} \sigma^{|l|+1} \right) \exp(-r^2/w_0^2 \sigma) \exp(ikz + il\varphi)$, where E_0 is the field amplitude, $\sigma = 1 + i(z/z_0)$, $z_0 = kw_0^2/2$ is the Rayleigh length, w_0 is the beam waist, and l is the vortex charge. For a partially coherent beam the correlation between different points of the wave front is diminished leading to the wash-out of the vortex core [25, 29, 31]. As a result, the far-field intensity distribution of a polychromatic vortex beam does not exhibit an on-axis intensity minimum.

It has been shown theoretically and experimentally [27, 28, 29] that circularly polarized coherent light beam propagating through the uniaxial crystal followed by a $\lambda/4$ plate and polarizer (Fig. 1) forms a beam with a topological charge $l = 2$ behind the plane of a polarizer. If, instead, the light passing through this system is partially coherent then the intensity distribution in a polarizer plane remains the same, as in the case of coherent radiation. This observation allows us to analyze the evolution of the intensity of partially coherent light in the region extended beyond the plane of the formation of the optical polychromatic vortex.

It is well known that if for any pair of points on a surface S across the beam of quasi-monochromatic light the mutual intensity is given, then it is always possible to determine it for each pair of points on any other surface S_1 illuminated by the light coming from S directly or via an optical system. We assume that the surface S corresponds to the surface of the polarizer in Fig. 1. Then the surface S_1 can be any plane parallel to S located behind the polarizer. The light intensity distribution on this surface can be found by employing the Huygens-Fresnel principle for partially coherent light [34].

$$I(P) = \int_S \int_S \sqrt{I(P_1)} \sqrt{I(P_2)} \gamma(P_1, P_2) \frac{\exp[2i\pi/\bar{\lambda}(s_1 - s_2)]}{s_1 s_2} \Lambda_1 \Lambda_2^* dP_1 dP_2, \quad (1)$$

where $\gamma(P_1, P_2)$ is the complex degree of coherence between points P_1 and P_2 on surface S , s_1

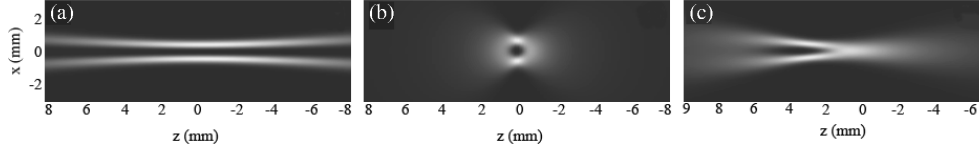


Fig. 4. Calculated longitudinal intensity distribution for (a) coherent, (b) highly incoherent, and (c) partially coherent (coherence angle $\alpha = 0.25$) vortex beams. Distance z_l between the vortex plane formation and the lens ($f=50$ mm) position is: (a,b) $z_l = 10f$, (c) $z_l = 3f$. Case (c) corresponds to the experimental results shown in Fig. 2.

and s_2 are the distances from the points P_1 and P_2 to the observation point P on the surface S_1 , Λ_1 and Λ_2 are the factors of an inclination of intervals s_1 and s_2 to surface S accordingly, $I(P_i)$ is the light intensity in point P_i on surface S . In the paraxial approximation $\Lambda \approx -i/\lambda$.

Using Eq. (1) directly is complicated by the fact that the complex degree of coherence $\gamma(P_1, P_2)$ and the corresponding intensity distribution $I(P_i)$ in the vortex plane (plane of polarizer) generally depends on position of this plane. However, this difficulty can be circumvented if the plane of the vortex formation lies in the immediate proximity of the exit pupil of an optical system. Assuming that the field intensity in the exit and entrance pupils are approximated by the Gaussian function, the intensity in the points on the surface immediately behind the polarizer can be represented in the form $I(P_i) = I_0[(x_i^2 + y_i^2)/w_s^2]^l \exp[-2(x_i^2 + y_i^2)/w_s^2]$, where w_s is the beam waist on the surface S . As each point P'_1 (P'_2) of the exit pupil is connected with the corresponding point P_1 (P_2) of an entrance pupil, then, in the paraxial approximation, the degree of coherence for these pairs of points coincide, and the phases of the corresponding values of complex degrees of coherence differ in magnitude $\Phi_{11} - \Phi_{22} = (2\pi/\lambda)[P_1\bar{P}'_1 - P_2\bar{P}'_2]$. Therefore, for any points of the exit pupil the complex degree of coherence can be written in the form: $\gamma(P'_1, P'_2) = 2[J_1(u)/u] \exp[i(\Phi_{11} - \Phi_{22})]$, where $u = (2\pi/\lambda)\Delta x \sin \alpha$, Δx is the distance between the points P'_1 and P'_2 , α is the angle under which the radius of the image of a source is visible from the center of the exit pupil of the system. Assuming that distances between the points are small enough in comparison with the distance between the planes of the entrance and exit pupils of the system and the displacement of phases of a wave in a crystal, we write

$$\gamma(P'_1, P'_2) = \frac{2J_1(u)}{u} \frac{(x_1 + iy_1)^{|l|}(x_2 - iy_2)^{|l|}}{(x_1^2 + y_1^2)^{|l|/2}(x_2^2 + y_2^2)^{|l|/2}}, \quad (2)$$

where (x_1, y_1) and (x_2, y_2) are the coordinates of the points P'_1 and P'_2 in the vortex plane. Equations derived above describe the formation of a *partially coherent vortex*. In the case when the beam is collimated well enough after the exit pupil, the parallel displacement of the plane of a polarizer does not produce an essential impact on the degree of coherence and intensity of the generated beam. To generate a bottle beam with a dark focal area, it is necessary to transfer the image of the vortex plane to the region of the geometrical focus of a lens. In order to evaluate the resulting light intensity distribution, the multipliers $[\exp(i\bar{k}_s)/s]\Lambda$ should be expressed in terms of the corresponding transmission function of the optical system [35]. The results are presented in Fig. 4, and they show that a dark area appears in the beam under the condition when the focusing lens is placed at the distance larger than the lens focus, $z > f$. The agreement between the calculations presented in Fig. 4(c) and the experimental data of Fig. 2 is excellent.

In conclusion, we have demonstrated a novel experimental method for generating linearly polarized optical bottle beams by double-charge white-light optical vortices. We have shown that the size and uniformity of the light intensity distribution around the dark area of the incoherent bottle beam is determined by the initial structure of the vortex.

This work was supported by the Australian Research Council.